RSC Advances

PAPER

View Article Online
View Journal | View Issue

Check for updates

Cite this: *RSC Adv.*, 2020, **10**, 1361

Excellent performance of aromatic polyguanamines induced by multiple hydrogen bondable tetraazacalix[2]arene[2]-triazine ring in their main chain†

H. Sasaki,[a] T. Kotaki,[a] A. Fujimori,[b] T. Tsukamoto,[a] E. Suzuki,[a] Y. Oishi[a] and Y. Shibasaki *[a]

A series of poly(guanamine) (*c*-PG)s containing tetraazacalix[2]arene[2]-triazine (*m*PDA$_2$CyC$_2$) were successfully prepared by solution polycondensation of *m*PDA$_2$CyC$_2$ with various aromatic diamines in an aprotic organic solvent with a lithium chloride additive (5 wt%) at 150 °C for 6 hours. The number-average molecular weights (M_n)s of these *c*-PG polymers reached up to 31 500, with a relatively broad molecular weight distribution (M_w/M_n) of 5.3. They showed good solubility in aprotic organic solvents, such as *N*-methylpyrrolidone and *N*,*N*-dimethylacetamide at a concentration of 2 mg mL^{-1}. The glass transition temperatures (T_g) of the *c*-PG polymers were in the range 359 °C–392 °C, approximately 160 °C higher than those of counterpart polymers (*i.e.*, with no aza-calixarene-based PG (*l*-PG)). The coefficients of thermal expansion (CTEs) of the *c*-PG polymers were 29.7–48.1 ppm K^{-1} (at 100 °C–150 °C), much lower than those of *l*-PG samples, *i.e.*, 59.1–85.1 ppm K^{-1}. Transparent and almost colorless *c*-PG films were successfully prepared by a solution casting method, showing maximum tensile strength (σ_S), modulus (E_γ), and elongation at break (E_b) values of 151 MPa, 6.3 GPa, and 4.4%, respectively, for the *c*-PG polymer from *m*PDA$_2$CyC$_2$ and 4,4′-oxydianiline monomers. The corresponding *l*-PG film exhibited σ_S, E_γ, and E_b values of just 76 MPa, 5.4 GPa, and 1.6%, respectively. These outstanding thermal and mechanical properties of the *c*-PG polymers can be attributed to their multiple hydrogen bonding interaction between *m*PDA$_2$CyC$_2$ residues in the polymer backbone. This interaction was identified by infrared spectroscopy measurements at the broad absorption band around 3000–3400 cm^{-1}.

Received 5th November 2019
Accepted 19th December 2019

DOI: 10.1039/c9ra09136j

rsc.li/rsc-advances

Open Access Article. Published on 08 January 2020. Downloaded on 6/14/2026 1:09:49 PM.
This article is licensed under a Creative Commons Attribution-NonCommercial 3.0 Unported Licence.

Introduction

For decades, attention has been paid to the synthesis of polymers having a cyclic skeleton, such as crown ethers,[1–6] cyclodextrins,[7] and calixarenes,[8] for application to ion recognition, separation, batteries, and supramolecular chemistry. Among them, calixarenes have been attracted great attention because of their rich functionalization chemistry and the well-defined molecular recognition capabilities.[9,10] There are a number of reports on the synthesis of polymers having calix[4]arenes as a bulky pendant group in the polymer backbone to study their metal coordination abilities.[11,12] Conjugated polymers are one of the hot research topics both in academic and industry, and calix[4]arenes were incorporated as a pendant side group, which enhanced the polymer solubility and was utilized as sensors toward various classes of molecules.[13–19] On the other hands, calixarenes are known to have a rigid structure, making their incorporation into a polymer backbone relatively difficult unless flexible solubilizing groups are introduced at the same time. Dondoni *et al.* synthesized a bisphenol A-type polymer having a calix[4]arene moiety in its main chain and studied Ag ion recognition.[20] Kim *et al.* reported the synthesis of rigid polyimides containing 25,26,27,28-tetrapropoxycalix[4]arenes in the backbone; however, the effect of the incorporation of the calix[4]arene moiety was not adequately revealed probably because of the tightly packed nature of the parent polyimide backbone.[21] Swager *et al.* reported the synthesis of polythiophene having 25,27-dimethoxy and 25,57-dipropoxycalix[4]arene and studied the spatial relationship between the electroactive polythiophene segments in terms of the electronic, optical, and optoelectronic properties.[22] They also reported the synthesis of main chain *p-tert*-butylcalix[4]arene base polymers utilizing acetylene coupling polymerization.[23] This *p-tert*-butylcalix[4]arene component was utilized for ring-opening metathesis copolymerization with cyclic alkenes, producing novel

[a]*Department of Chemistry & Biological Sciences, Faculty of Science & Engineering, Iwate University, 4-3-5 Ueda, Morioka, Iwate 020-8551, Japan. E-mail: yshibasa@iwate-u.ac.jp*

[b]*Graduate School of Science and Engineering, Saitama University, 255 Shimo-okubo, Sakura-ku, Saitama 338-8570, Japan*

† Electronic supplementary information (ESI) available. See DOI: 10.1039/c9ra09136j

Open Access Article. Published on 08 January 2020. Downloaded on 6/14/2026 1:09:49 PM.
This article is licensed under a Creative Commons Attribution-NonCommercial 3.0 Unported Licence.

elastomers in which the calixarene and polyalkene components were functioned as hard and soft segments, respectively.[24] Recently, novel aza- and/or oxo-bridged calix[2]arene[2]triazine derivatives with 1,3-alternative conformation were developed by Wang *et al.*, and the structures were found to be the roughly coplanar two-triazine rings with almost perpendicular (to the planes) benzene rings defined by four bridged heteroatoms.[25] Tuning of the cavity made by the calixarene moiety enabled them to work as fluorine sensors.[26]

Cyanuryl polyimines, known as poly(guanamine)s (PG)s, are condensation polymers. They are usually prepared from triazine dichloride and diamine monomers in solution, with a variety of derivatives having been synthesized to date.[27–34] The guanamine functional group was also found in Wang's aza-bridged calix[2]arene[2]triazine (*m*PDA_2CyC_2), which has two active C–Cl bonds; therefore, we expected that a *m*PDA_2CyC_2 residue would exhibit a unique effect on PG structure. In particular, if rigid aromatic diamines were combined with *m*PDA_2CyC_2 during polycondensation, then a new series of condensation polymers having a tightly packed structure should be obtained. Our motivation in this research was in uncovering the unique and original nature of *m*PDA_2CyC_2-based PG polymers (*c*-PG), particularly in terms of thermal and mechanical properties, which can be significantly affected by the multiple hydrogen bonding abilities of *m*PDA_2CyC_2. As counterpart polymers, we also prepared non-calixarene-type PG polymers (*l*-PG), for which we compared the physical properties with those of the *c*-PG polymers. Herein, we report the synthesis and properties of novel azacalixarene containing *c*-PGs, utilizing *m*PDA_2CyC_2 as a cyclic guanamine monomer.

Results and discussion

Monomer and polymer synthesis

Cyclic guanamine calixarene (*m*PDA_2CyC_2) was prepared in accordance with Wang's method;[25] the structure was confirmed by NMR and FAB MS spectroscopy (Scheme S1, Fig. S1–S3†). First, *l*-PG was prepared as a non-azacalixarene-type polymer in accordance with the literature.[32] For instance, poly(AnDCT-*m*PDA) [*l*-PG(*m*PDA)] was prepared by solution polycondensation of AnDCT with *m*PDA in NMP (total monomer concentration was 1.0 mol L^{-1}); 65% yield, $M_n = 5000$, $M_w/M_n = 3.6$ (Run 7, Table 1). Relatively low M_n of the polymer is attributable to the low solubility of *l*-PG(*m*PDA) with accompanying the formation of cyclic oligomers due to the *meta* phenylene linkage. By spontaneous polycondensation of AnDCT with *m*PDA and the corresponding diamine comonomers, the other *l*-PG polymers were prepared with reasonable M_n (Runs 8 and 9). In accordance with a similar procedure, the synthesis of *c*-PGs was then attempted using *m*PDA_2CyC_2 with various aromatic diamine monomers; however, the polymerization solution instantly became a gel within the reaction time. Therefore, polymerization was conducted in more dilute conditions (0.060 to 0.40 mol L^{-1} for *m*PDA_2CyC_2 depending on the diamine monomers used) with 5 wt% LiCl as a solubilizer at 150 °C for 6 hours (Scheme 1). To avoid gelation, the synthesis of *c*-PG polymers consisting of rigid diamine monomers, such as *p*PDA, required highly dilute conditions of below 0.10 mol L^{-1} for *m*PDA_2CyC_2. Thus, the final obtained M_n was only 6300, with a low polymer yield of 55% (Run 1, Table 1). However, diamine monomers having a bent structure or a bulky pendant group resulted in the formation of high-M_n polymers with good yields (Runs 2–5, Table 1). These higher M_n values of *c*-PGs compared with those of *l*-PGs can be explained by avoiding cyclic oligomer formation. For *l*-PG synthesis, although the addition of LiCl did not significantly improve the M_n values of the polymers, the corresponding films could be prepared (Runs 10–12, Table 1).

Fig. 1 shows the FT-IR spectra of the prepared polymers. Owing to the comparable structures of *c*-PG and *l*-PG (as illustrated in Fig. 2), their IR spectra appear almost identical, except for the shoulder peak at 3370–2800 cm^{-1}, which results from the multiple hydrogen bonding absorption at the guanamine moiety, as reported in the literature.[35] The absorption at 3616 cm^{-1} can be assigned to free guanamine NH stretching vibration and was only observed for *c*-PG polymers. The absorptions at 3377 and 3370–2800 cm^{-1} can be assigned to

Table 1 Synthesis of *c*- and *l*-PG polymers[a]

Run	Polym.	Add.	$[m\text{PDA}_2\text{CyC}_2]_0$ (mol L^{-1})	*Y* (%)	M_n[b] (kDa)	M_w/M_n[b]	Film[c]
1	*c*-PG (*p*PDA)	LiCl	0.060	55	6.3	5.0	X
2	*c*-PG (*m*PDA)	LiCl	0.20	85	26.0	3.2	F
3	*c*-PG (ODA)	LiCl	0.20	91	24.3	7.1	F
4	*c*-PG (BAFL)	LiCl	0.25	92	24.9	7.3	F
5	*c*-PG (TFMB)	LiCl	0.22	83	30.5	4.4	F
6	*c*-PG (BisAAF)	LiCl	0.40	84	31.5	5.3	B
7	*l*-PG (*m*PDA)	—	1.0	65	5.0	3.6	X
8	*l*-PG (BAFL)	—	1.0	81	10.4	3.7	B
9	*l*-PG (*p*PDA)	—	1.0	80	11.6	3.5	B
10	*l*-PG (*m*PDA)	LiCl	1.0	66	7.3	3.8	B
11	*l*-PG (BAFL)	LiCl	1.0	76	13.4	4.2	B
12	*l*-PG (ODA)	LiCl	1.0	79	9.3	6.4	B

[a] Conditions; in NMP at 150 °C for 6 h for *c*-PG and at 110 °C for 9 h for *l*-PG. [b] Determined by GPC (NMP, PS standards). [c] X: free-standing film cannot be prepared, B: brittle film, F: flexible film.

 This journal is © The Royal Society of Chemistry 2020

Open Access Article. Published on 08 January 2020. Downloaded on 6/14/2026 1:09:49 PM.
This article is licensed under a Creative Commons Attribution-NonCommercial 3.0 Unported Licence.

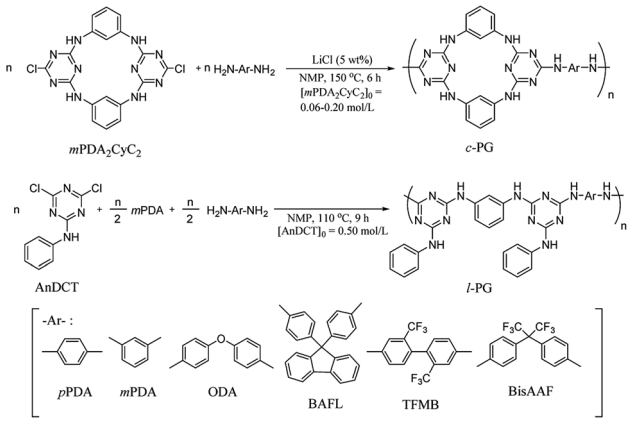

Scheme 1 Synthesis of *c*- and *l*-PG polymers.

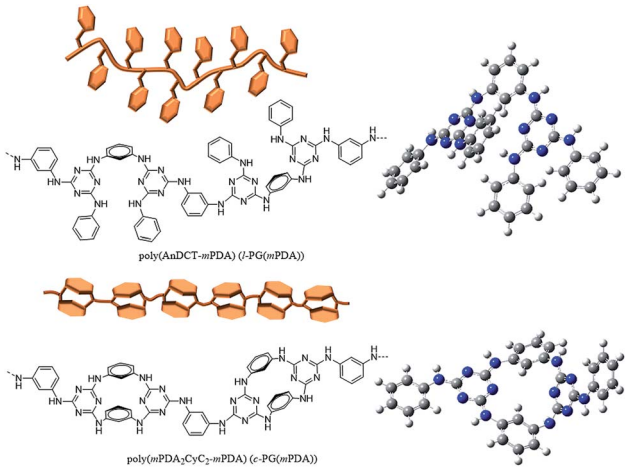

Fig. 2 Chemical structures, illustration, and optimized geometries of poly(AnDCT-*m*PDA) (*l*-PGA(*m*PDA)) (upper) and poly(*m*PDA$_2$CyC$_2$-*m*PDA) (*c*-PGA(*m*PDA)) (lower) as representatives of *l*- and *c*-PG polymers. The calculation was performed with the Gaussian 03W program and the Hartree–Fock method using the basis set of the 3-21G function.

hydrogen-bonded NH stretching and multiple hydrogen-bonded NH stretching, respectively. The absorption at 1441 cm^{-1} can be assigned to a multiple hydrogen-bonded C=N group, which is clearly observed, especially for *c*-PG samples. To study more about multiple hydrogen bond interactions between polymer chains, the FT-IR spectra of the PG polymer powder mixed with KBr were recorded at temperatures ranging from 20 to 200 °C (Fig. 3). As the temperature increased, the absorption intensities all decreased. These changes were not reversible even when the heated sample was cool down to room temperature. The most relevant changes were observed at 3000 to 3500 cm^{-1}, which could be attributed to both the moisture desorption within polymer chains and the development of hydrogen bonding network.

Wang *et al.* performed temperature variable FT-IR study of diaminotriazine derivatives, in which clear decrease of the absorption at 3273 cm^{-1} (hydrogen bonded NH) was observed against that at 3379 cm^{-1} (free NH) especially above 54 °C that is the T_g of the samples.[35] And these absorption changes were reversible with temperature. In contrast, our PG polymer samples only showed the absorption decrease, and the intensities were not recovered with temperature. These indicates that our *l*- and *c*-PG polymer samples should have high T_g above the FT-IR spectra measurement conditions of 200 °C. On the other hands, there are clear differences between the spectra from 3000 to 3500 cm^{-1}, between *l*- and *c*-PG samples. The initially observed absorption at 3500 cm^{-1} of *c*-PG sample at 20 °C is much larger than that of *l*-PG, and in the spectrum of *c*-PG the shoulder peak at 3000 to 3300 cm^{-1} are more clearly observed

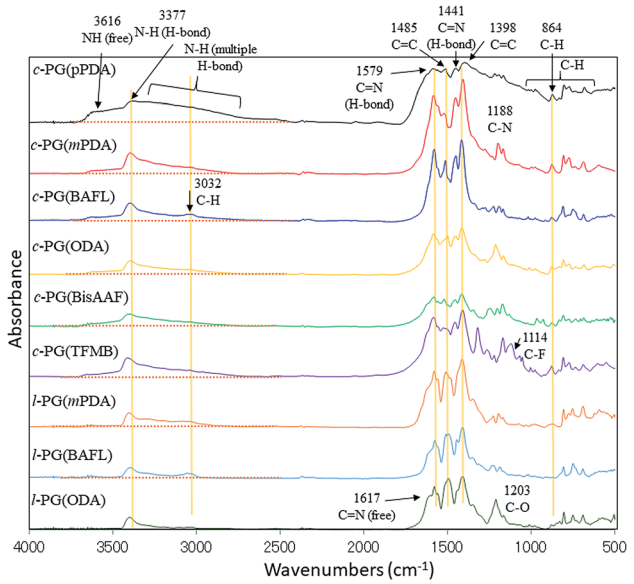

Fig. 1 FT-IR spectra of the prepared polymers (KBr method).

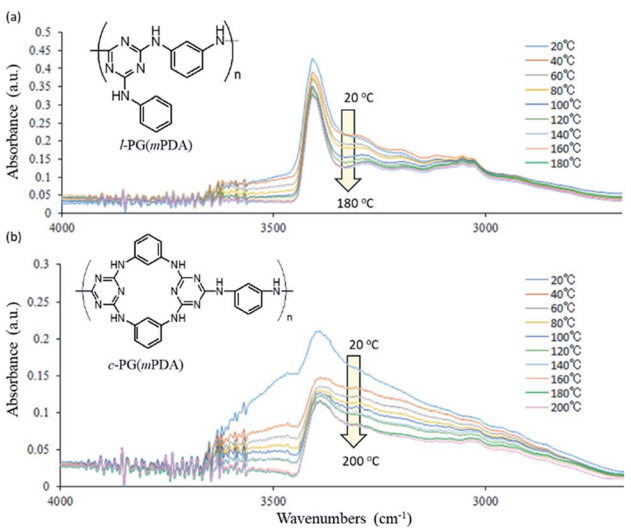

Fig. 3 Expanded FT-IR spectra changes of (a) *l*-PG(*m*PDA) and (b) *c*-PG(*m*PDA) heated from 20 to 200 °C.

Open Access Article. Published on 08 January 2020. Downloaded on 6/14/2026 1:09:49 PM.
This article is licensed under a Creative Commons Attribution-NonCommercial 3.0 Unported Licence.

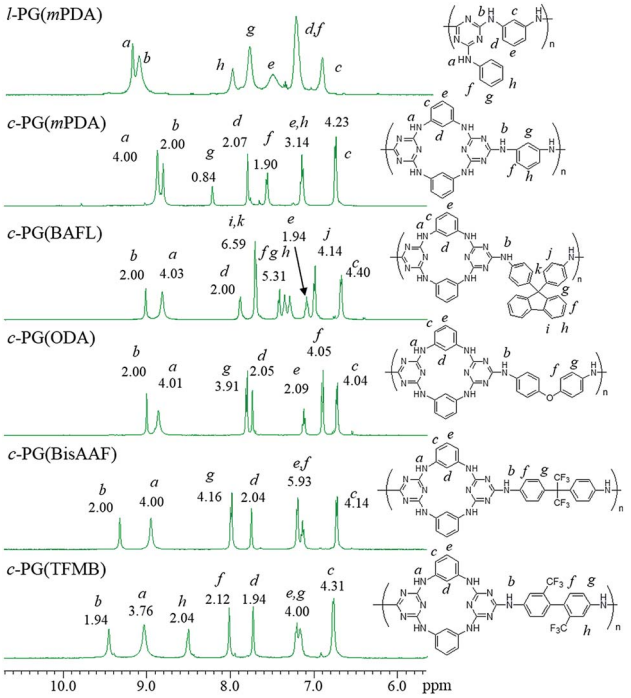

Fig. 4 ^{1}H NMR spectra of *c*- and *l*-PG samples in DMSO-d_6.

even after heated to 200 °C. These suggests that *c*-PG polymers initially have some weak hydrogen bonding interaction between polymer chains, and these be developable with heating. In our current method to study FT-IR spectra, the attainable measurable temperature using heated sample was up to 200 °C that is far below the T_g of PG samples (220 °C for *l*-PG(*m*PDA) and 370 °C for *c*-PG(*m*PDA)), and thus the reversible FT-IR spectra changes were not observed.

The optimized geometry of the *c*-PG and *l*-PG models was determined with the Gaussian 03W program and the Hartree–Fock method, using the basis set of the 3-21G function (Fig. 2, right). The meta-linked bent structure of the *l*-PG polymer backbone based on mPDA$_2$CyC$_2$ and *m*PDA, together with the pendant aniline substituent, make the polymer structure cramped. On the contrary, the *m*PDA unit is covalently bonded at both sides in the *c*-PG polymer backbone; therefore, the *c*-PG polymer is free from the steric repulsion of the pendant aniline group. According to Wang's X-ray crystallographic study, mPDA$_2$CyC$_2$ has a boat-like geometry with two *m*PDA units and two-triazine rings.[25] As a result, the mutually connected mPDA$_2$CyC$_2$ and *m*PDA monomer molecules make the *c*-PG polymer structure more extendable and flat, which significantly increase the hydrogen bonding opportunities between the polymer chains. These spectroscopic data and calculation results indicate that owing to multiple hydrogen bondable sites, the azacalixarene guanamine moieties are more tightly packed in the *c*-PG structure than they are in the linear structure of *l*-PG polymers.

Fig. 4 shows the expanded ^{1}H NMR spectra (from 6 to 11 ppm) of the prepared polymers (full spectra are given in the ESI as Fig. 4s†). The *l*-PG polymer (*l*-PGA(*m*PDA)) shows a typically broad signal observed at 7.50 (e) ppm, assignable to the *m*PDA unit. This is a result of the rotation limitation of the phenyl ring, which is caused by the weak hydrogen bonding between aromatic C–H (d) and triazine nitrogen. The guanamine protons are observed at 9.18 (a, 1H) and 9.10 (b, 2H) ppm. For the corresponding *c*-PG sample (*c*-PG(*m*PDA)), the proton labelled as h, assignable to the phenyl ring moiety of *m*PDA, is observed at 7.20 ppm, with proton e presenting as a sharper signal. The *m*-phenylene linkage in *c*-PG has more freedom in its rotation in solution. In addition, the electron density of the triazine moiety is higher than that in *l*-PG because of the additional introduction of the *m*-phenylenediamine group.

Molecular orbital calculation study

Although the structural similarity of the *l*- and *c*-PG polymers as explained in Fig. 2, both of the IR and NMR measurements gave the slightly different spectra. To study the relationship between the structure and the properties, the time dependent density functional theory (TD-DFT) was applied for the model compounds of the prepared polymers. Fig. 5 depicts the optimized geometry of the model compounds for *l*-PG(*m*PDA) and *c*-PG(*m*PDA) with the illustrations of the molecular orbitals. For the *l*-PG(*m*PDA) model, there were several minimum excited states such as from n = 154 to 166, and the band gap energy was calculated to be 5.31 eV (λ = 233.5 nm). On the other hands, the *c*-PG(*m*PDA) model showed larger band gap energy of 5.94 eV (λ = 208.4 nm). The corresponding molecular orbitals of the two model compounds indicate that the HOMO of the *c*-PG(*m*PDA) model is uniformly more delocalized at the azacalixarene moiety thanks to the coplanarity of the azacalixarene skeleton, which might enlarge the band gap energy of the *c*-PG polymer. From these calculation results, we expected that the *c*-PG polymer should have higher thermal, mechanical, and optical properties due to the accessible azacalixarene flat rings within the polymer chains.

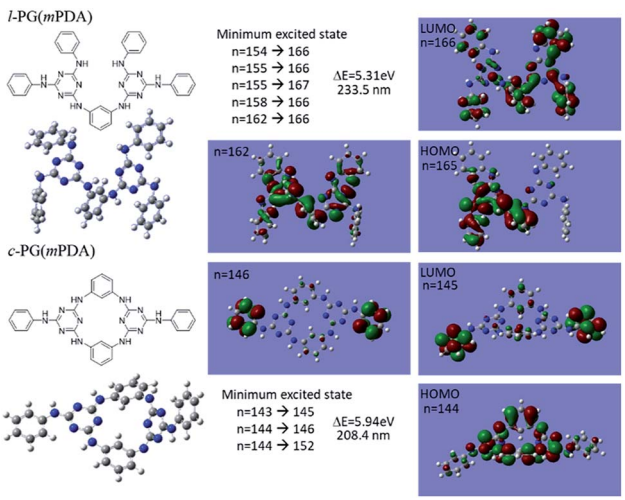

Fig. 5 Optimized geometry of model compounds for *l*-PG(*m*PDA) and *c*-PG(*m*PDA) with the molecular orbital illustrations as obtained from DFT/Hartree–Fock 3-21G level of calculation.

This journal is © The Royal Society of Chemistry 2020

Open Access Article. Published on 08 January 2020. Downloaded on 6/14/2026 1:09:49 PM.
This article is licensed under a Creative Commons Attribution-NonCommercial 3.0 Unported Licence.

Polymer properties

The solubility values of the prepared *c*-PG polymers are summarized in Table 1s.† These polymers are soluble only in aprotic polar solvents, such as DMAc and NMP, at 25 °C and at 2 mg mL^{-1} concentration; they are insoluble in THF, $CHCl_3$, γ-butyrolactone, propylene glycol monomethyl ether, and cyclohexanone. The rigid-rod polymer *c*-PG(*p*PDA) is only soluble in DMAc and NMP and is partially soluble in DMF and DMSO upon heating, which agrees with the observation that the polymer was precipitated even during polymerization.

The thermal properties of the *c*- and *l*-PG polymers were evaluated by TG/DTA, DSC, TMA, and DMA. Table 2 summarizes the glass transition temperatures (T_gs) measured by DMA, the 5 and 10 wt% weight loss temperatures (T_{d5} and T_{d10}), and the char yield at 800 °C measured by TG. The T_g values of the *c*-PG samples range from 359 °C to 392 °C, approximately 160 °C higher than those of the reference *l*-PG polymers. The T_{d5} and T_{d10} data also illustrate the higher thermostability of the *c*-PG samples. These physical and chemical thermostabilities can be attributed to the azacalixarene moieties.

Fig. 6 depicts the DMA profiles of the *c*- and *l*-PG films dried at 150 °C for 12 hours. The *l*-PG(ODA) film initially showed a storage modulus E' (E_0') of 1.72 GPa. This value started to sharply decrease from 137 °C (T_s), reaching a rubbery plateau from 228 °C (T_r) at an E' value (E_r') of 0.0135 GPa. For the *l*-PG(BAFL) film, the DMA curve showed better thermal stability owing to its rigid and bulky fluorene pendant effect, *i.e.*, the values of T_s, T_r, E_0', and E_r' were 199.7 °C, 288.8 °C, 4.79 GPa, and 0.0257 GPa, respectively. For the *c*-PG films, the values of T_s, T_r, E_0', and E_r' were significantly improved to 372.4 °C, 423.6 °C, 5.18 GPa, and 0.506 GPa for *c*-PG(ODA) and 387.1 °C, > 425.5 °C, 5.98 GPa, and > 0.615 GPa for *c*-PG(BAFL), respectively. The plot of tan δ and measured temperature for the *l*-PG(ODA) film shows two peaks at 177.1 °C and 204.5 °C, indicating that the polymer main chain produced a more stable packed structure with thermal agitation. The peaks show the T_g values of the polymers, reaching 0.8 and 1.6 for *l*-PG(ODA) and *l*-PG(BAFL), respectively. For the *c*-PG films, the tan δ profiles also show two peaks at 286.4 °C and 360.6 °C for *c*-PG(ODA) and at 259.4 °C and >424.0 °C for *c*-PG(BAFL). However, these peaks show maximum values of only 0.1059 for *c*-PG(ODA) and 0.0510 for *c*-PG(BAFL). These very small tan δ values indicate the absence of an E'' contribution, which clearly suggests the dominant elastic nature of the *c*-PG polymers, with multiple densely bound hydrogen bonds at the azacalixarene moiety.

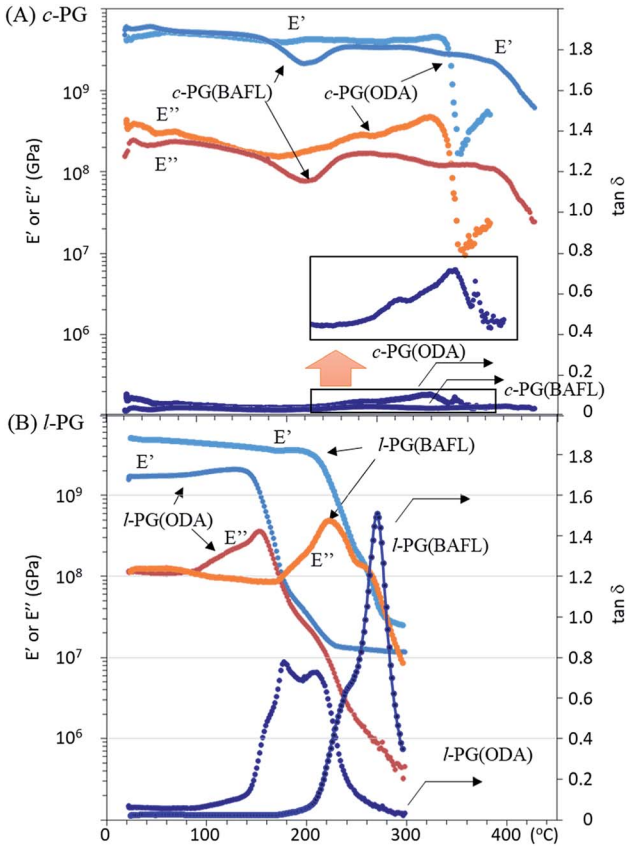

Fig. 6 DMA profiles of (A) *c*-PG and (B) *l*-PG films.

Fig. 7 depicts the TMA profiles of the *c*- and *l*-PG(BAFL) films. The shape of the *l*-PG(BAFL) film gradually changed and started to markedly expand at 238.9 °C. By contrast, the *c*-PG(BAFL) film mostly retained its shape within the measured temperature range up to 380 °C, indicating the effectiveness of azacalixarene

Table 2 Thermal properties of *c*- and *l*-PG polymers[a]

	T_g (°C)			T_{d5}[a] (°C)	T_{d10}[a] (°C)	T_{d5}[a] (°C)	T_{d10}[a] (°C)		
Polymer	DSC	DMA	TMA	N_2		Air		Char[b] (%)	CTE[c] (ppm K^{-1})
c-PG (*m*PDA)	—[d]	368	372	506	542	444	448	61.8	48.10
c-PG (ODA)	—[d]	359	357	513	539	448	451	59.7	38.14
c-PG (BAFL)	—[d]	386	—	522	542	476	480	61.1	29.68
c-PG (BisAAF)	—[d]	—[d]	392	513	534	479	498	55.0	44.35
c-PG (TFMA)	—[d]	—[d]	374	496	523	471	489	54.4	39.37
l-PG (*m*PDA)	218	—[d]	—[d]	416	436	404	432	50.2	—[d]
l-PG (BAFL)	255	223	248	427	444	415	442	51.9	59.07
l-PG (ODA)	206	154	163	432	452	452	469	56.3	85.09

[a] Determined by TGA (10 °C min). [b] Char yield at 800 °C. [c] Determined by TMA from 100–150 °C. [d] Not detected.

Open Access Article. Published on 08 January 2020. Downloaded on 6/14/2026 1:09:49 PM.
This article is licensed under a Creative Commons Attribution-NonCommercial 3.0 Unported Licence.

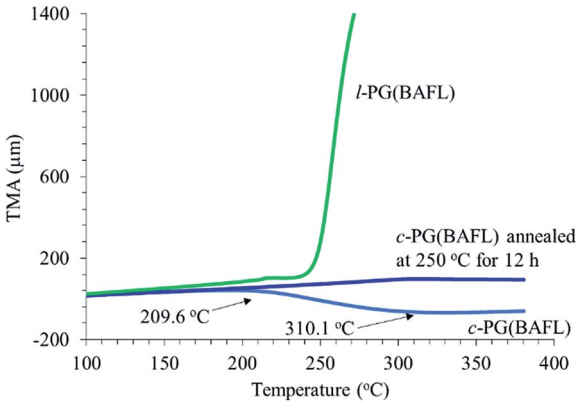

Fig. 7 TMA profiles of *c*- and *l*-PG films.

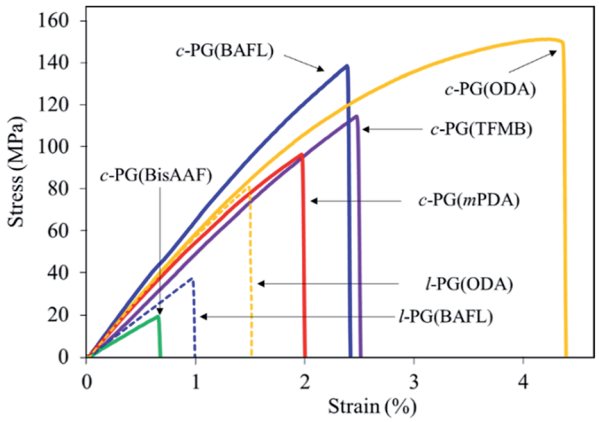

Fig. 8 Tensile properties of PG films.

packing. However, during TMA measurement, the *c*-PG(BAFL) film shrank from 209.6 °C to 310.1 °C, which was also observed for DMA (Fig. 6(A)). This may be caused by the reorientation of the polymer chains in the film upon thermal treatment. Pre-annealing of the film at 250 °C for 12 hours prevented such shrinkage, with the film retaining its shape above 380 °C. The CTE values were measured as 59.07 ppm K^{-1} for *l*-PB(BAFL) and 29.68 ppm K^{-1} for *c*-PB(BAFL) in the temperature range of 100 °C–150 °C. As illustrated in Fig. 2, as *l*-PG polymers have pendant aniline side groups that can freely rotate along with the polymer main chain, the film tended to become brittle even at a high molecular weight. By contrast, the *c*-PG polymers afford a flexible film and high thermal stability. This can be explained on the basis that the structure of the *c*-PG polymer is more extended and flat than that of the *l*-PG polymer. Moreover, the polymer main chains are functionalized with azacalixarene moieties, which can be further tightly packed with the multiple hydrogen bondable sites.

Table 3 and Fig. 8 summarize the mechanical properties of the polymer films. We first assumed that the *c*-PG films should have a higher modulus and thus be brittle in nature owing to the existence of azacalixarene moieties. However, the films we prepared were stronger than their linear counterparts (*i.e.*, the *l*-PG films), whose tensile strength (σ_{TS}), elongation at break (E_b), and tensile modulus (E_γ) values were 37.0–76.0 MPa, 1.0–1.6%, and 4.2–5.4 GPa, respectively. As observed in Fig. 8, the *l*-PG films broke only below a strain of 1.5%. This behaviour is generally observed for PG polymers having a bulky pendant group like an aniline function, which restricts the effective entanglement between polymer main chains (Fig. 2). Surprisingly, the *c*-PG films (except for *c*-PG(BisAAF)) show much better tensile properties (σ_{TS} = 96–151 MPa, E_b = 2.0–4.4%, E_γ = 5.2–7.0 GPa), probably owing to the more extended and flat polymer backbone without freely rotatable aniline substituents, and stronger interaction between azacalixarene moieties. As observed in DMA and TMA analyses, the polymer main chains can be rearranged with outer stimuli. Therefore, assisted by azacalixarene interaction, the *c*-PG films are able to change their polymer chains in a manner suitable for enduring the outer load.

Table 3 Tensile properties of PG polymers

Run	Polym.	Thickness (μm)	σ_{TS}[a] (MPa)	E_b[b] (%)	E_γ[c] (GPa)
1	*c*-PG(*m*PDA)	15.0	96.0	2.0	5.9
2	*c*-PG(ODA)	10.3	151	4.4	6.3
3	*c*-PG(BAFL)	16.2	138	2.4	7.0
4	*c*-PG(TFMB)	8.2	114	2.5	5.2
5	*c*-PG(BisAAF)	21.0	19.0	0.7	3.1
6	*l*-PG(BAFL)	70.4	37.0	1.0	4.2
7	*l*-PG(ODA)	47.2	76.0	1.6	5.4

[a] Tensile strength. [b] Elongation at break. [c] Tensile modulus.

The optical properties of the prepared polymer films were analyzed using a UV-vis spectrophotometer and prism coupler, as summarized in Table 4 and Fig. 9.

The *c*-PG films were slightly yellow in colour but were more colourless and transparent compared with the *l*-PG films. The M_n values of the *l*-PG polymers were 7300–13 400 and showed slightly better solubility in the aprotic solvent. However, the tensile and optical properties of *l*-PG polymers were obviously inferior to those of the *c*-PG films.

The refractive index (n) was measured by a prism coupler, and the results are summarized in Table 4. The PG films generally show a high refractive index (n_{594}) of approximately 1.7 and low Abbe number (ν) owing to their tight packing and the high molecular refraction of the triazine component. *l*-PG(ODA) and *l*-PG(BAFL) showed average n_{594} values of 1.7114 and 1.7309, respectively, whereas the *c*-PG counterpart films showed values of 1.7417 and 1.7337, respectively. The slightly higher n_{594} values can be attributed to the azacalixarene moieties. The ν values of the *c*-PG films were larger than those of the *l*-PG films. These results can be explained by the strong interaction with azacalixarene, which somehow regulates the chain motion of the polymers in the film.

Table 5 summarizes the major properties of PG polymers categorized in their skeleton. As a solubilizing group, an alicyclic pendant such as adamantly group (AdDCT) is somewhat effective with keeping the thermal stability, but the n_{594} of the brittle thin film is only 1.672 (for BAFL).[32] Simple anilino

This journal is © The Royal Society of Chemistry 2020

Open Access Article. Published on 08 January 2020. Downloaded on 6/14/2026 1:09:49 PM. This article is licensed under a Creative Commons Attribution-NonCommercial 3.0 Unported Licence.

Table 4 Optical properties of PG polymers

Polymer	Thickness (μm)		n^a 473 nm	594 nm	657 nm	ν^b	Δn^c	$n_{ave}{}^d$
c-PG (*m*PDA)	13.0	TE	1.8251	1.7819	1.7679	15	0.0754	1.7571
		TM	1.7357	1.7065	1.6957	20		
c-PG (BAFL)	12.0	TE	1.7839	1.7476	1.7352	17	0.0421	1.7337
		TM	1.7347	1.7055	1.6953	20		
c-PG (ODA)	9.0	TE	1.8078	1.7677	1.7538	16	0.0793	1.7417
		TM	1.7154	1.6884	1.6786	21		
c-PG (BisAAF)	11.0	TE	1.7237	1.6916	1.6817	19	0.0572	1.6728
		TM	1.6560	1.6344	1.6255	23		
c-PG (TFMA)	11.0	TE	1.7398	1.7050	1.6938	17	0.0844	1.6773
		TM	1.6413	1.6206	1.6130	24		
l-PG (BAFL)	71.0	TE	1.7666	1.7339	1.7218	18	0.0090	1.7309
		TM	1.7498	1.7249	1.7129	20		
l-PG (ODA)	47.0	TE	1.7429	1.7133	1.7007	19	0.0058	1.7114
		TM	1.7349	1.7075	1.6959	20		

[a] TE, in-plane; TM, out-of-plane. [b] Abbe's number. [c] Birefringence at 594 nm. [d] $n_{ave} = ((2 \times n_{TE}{}^2 + n_{TM}{}^2)/3)^{0.5}$: n_{TE} and n_{TM} measured at 594 nm were used.

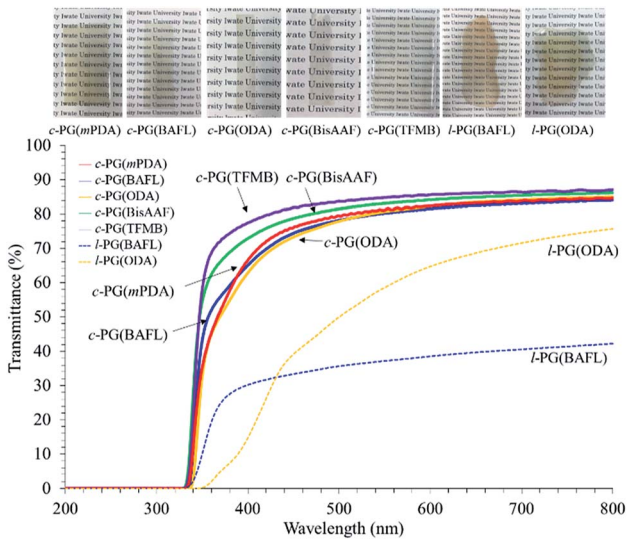

Fig. 9 UV-vis spectra of PG films.

pendant in AnDCT is more effective to suppress over-aggregation, so the soluble transparent high M_n polymers are successfully obtained when BAFL is used to avoid cyclization.[32] T_g of the polymer is 287 °C, and its n_{594} is improved up to 1.709. Semiaromatic-type PG polymers using α,ω-alkylene diamines as monomers generally show poor solubility in organic solvents with the strong aggregation and the packing caused by crystalline nature, which cause low transparency in the state of film.[34] In order to secure the solubility, longer alkylene diamine segment such as DDDA is required, but the prepared polymer shows poor thermal stability (low T_g of 76 °C, low T_{d5} of 438 °C, and low char at 800 °C of only 7.0%). This can be caused by the weak packing of alkylene chain with the low weight fraction of triazine moiety. The film is relatively low transparency with low n_{594} of 1.616. In contrast with the above mentioned PG polymers, the *c*-PG polymers developed in this study showed good solubility in aprotic polar organic solvents, and the formation of the cyclic oligomer during the polymerization process be effectively avoidable. Extraordinary high thermal stabilities (T_g > 380 °C, T_{d5} > 520 °C, and char at 800 °C > 61%) with excellent

Table 5 Properties of PG polymers categorized in the skeleton

PG type	Dichloride[a]	Diamine[b]	$M_n{}^c$ (kDa)	T_g (°C)	$T_{d5}(N_2)$ (°C)	Char (%)	$n_{594}{}^f$
Alkyl side pendant	AdDCT	*m*PDA	3.6	271[d]	430	47.0	—
		BAFL	13.5	347[d]	468	52.0	1.672
Semiaromatic	AnDCT	HMDA	(Insoluble)	161[d]	405	20.7	—
		DDDA	68.0	76[d]	438	7.0	1.616
Wholly aromatic	AnDCT	*m*PDA	3.1	209[d]	418	58.0	1.783
		BAFL	36.1	287[d]	448	54.5	1.709
c-PG	$mPDA_2CyC_2$	*m*PDA	26.0	368[e]	506	61.8	1.757
		BAFL	24.9	386[e]	522	61.1	1.734

[a] AdDCT: adamantylamino-*s*-triazine dichloride. [b] HMDA: hexamethylene diamine, DDDA: dodecylene diamine. [c] Determined by GPC (NMP, PS standards). [d] Determined by DSC. [e] Determined by DMA. [f] Refractive index at 594 nm.

Open Access Article. Published on 08 January 2020. Downloaded on 6/14/2026 1:09:49 PM.
This article is licensed under a Creative Commons Attribution-NonCommercial 3.0 Unported Licence.

optical properties ($\lambda_{cut\ off}$ 332 nm, $n_{594} > 1.75$) should be the gifts from the cyclic skeleton of mPDA$_2$CyC$_2$ group with its dense packing utilizing its multiple hydrogen bondable ability.

Conclusions

In this study, we successfully synthesized a series of high molecular weight poly(guanamine) (*c*-PG)s containing an azacalixarene moiety. We revealed their outstanding thermal, mechanical, and optical properties and compared them with their linear counterparts (*l*-PG). Introducing multiple hydrogen bondable units of the azacalixarene moiety into the polymer skeleton provided elastomeric exclusively to the polymers, affording these unusual properties. We believe that our findings from this research will be applicable to the design and synthesis of a novel series of ring-containing polymers and materials.

Experimental

Materials

Cyanuric chloride (CyC) (TCI Chemical), *N*,*N*-diisopropylethylamine (DIPA) (Kanto Chemical), and ammonium hydroxide solution in water (Wako Pure Chemical) were purchased and used as received. *m*-Phenylene diamine (*m*PDA), *p*-phenylene diamine (*p*PDA), and 4,4′-oxydianiline (ODA) were purchased from TCI Chemical and purified *via* sublimation. 9,9-Bis(4-aminophenyl)fluorene (BAFL) was purified *via* recrystallization from ethanol before use. 2,2′-Bis(trifluoromethyl)benzidine (TFMB) and 2,2-bis(4-aminophenyl)hexafluoropropane (BisAAF) were purchased from TCI Chemical and used as received. 2-Anilino-4,6-dichloro-1,3,5-triazine (AnDCT) was prepared by the method given in our previous report.[32] *N*-Methylpyrrolidone (NMP) was dried over calcium hydride (CaH_2) and distilled under reduced pressure prior to use. Anhydrous tetrahydrofuran (THF) was purchased from Wako Pure Chemical and used as received. All other reagents and solvents were used as received.

Synthesis of mPDA$_2$CyC$_2$

The compound mPDA$_2$CyC$_2$ was prepared by Wang's method.[25] Briefly, two equivalents of CyC were reacted with *m*PDA in the presence of DIPA in THF at −5 °C for 18 hours to give *N*,*N*′-bis(dichloro-*s*-triazinyl)-*m*-phenylenediamine (71% yield), which was further reacted with *m*PDA in acetone at 20 °C for 48 hours. The final product was purified by recrystallization with hexane–dichloromethane mixed solvent (45% yield). Mp > 300 °C (lit. [25], mp > 300 °C). FT-IR [KBr (cm^{-1})]: 3246 (N–H), 1596 (C=C), 1576 (C=N), 1558 (C=C), 1388 (C=C). ^{1}H-NMR (400 MHz, DMSO-d_6, ppm) δ 6.80 (dd, 4H, Ar-H), 7.23 (t, 2H, Ar-H), 7.76 (s, 2H, Ar-H), 10.01 (s, 4H, N–H). ^{13}C-NMR (100 MHz, DMSO-d_6, ppm) δ 118.2, 118.8, 129.0, 137.9, 164.3, 168.0. FAB-mass found: $m/z = 439.0702$ ($C_{18}H_{13}Cl_2N_{10}$) Err [ppm/mmu] = +3.7/+1.6.

Synthesis of linear-type PG (*l*-PG)

The typical procedure used for poly(AnDCT-*m*PDA) (*l*-PG(*m*PDA)) was as follows:[32] all of the glass vessels were heated under a vacuum before use and were filled with and handled in a stream of dry nitrogen. In a two-neck flask equipped with a three-way stopcock, reflux condenser, and magnetic stirrer, *m*PDA (0.216 g, 2.00 mmol) was dissolved in dry NMP (4 mL) containing lithium chloride (5 wt%) at room temperature. To this solution, AnDCT (0.482 g, 2.00 mmol) was added in one portion. The mixture was stirred for 10 min, followed by stirring at 110 °C for 9 hours. The polymerization solution was then cooled to room temperature and poured into an excess amount of methanol containing NH_3 (aq.) to remove HCl and inorganic salts produced during the reaction. The precipitate was dried at 60 °C for 12 hours, washed with hot methanol, and dried at 140 °C for 12 hours under reduced pressure. This procedure afforded the title polymer in 0.364 g (66%) yield. FT-IR [KBr (cm^{-1})]: 3385 (N–H), 3335–32 887 (N–H, H-bonded), 1625 (C=C), 1576 (C=N), 1500 (C=C), 1475 (C=C), 1441, 1406, 1365 (C=N), 1219, 1188, 1162 (C–N), 801, 767, 745, 686 (C–H). ^{1}H NMR (400 MHz, DMSO-d_6, ppm) δ 6.91 (aromatic CH, 1H), 7.22 (aromatic CH, 3H), 7.50 (aromatic CH, 1H), 7.78 (aromatic CH, 2H), 7.98 (aromatic CH, 1H), 9.10 (guanamine NH, 2H), 9.18 (aniline NH, 1H).

Synthesis of mPDA$_2$CyC$_2$ containing PG (*c*-PG)

The typical procedure used for poly(mPDA$_2$CyC$_2$-*m*PDA) (*c*-PG(*m*PDA)) was as follows: in a two-neck flask equipped with a three-way stopcock, reflux condenser, and magnetic stirrer, *m*PDA (0.108 g, 1.00 mmol), lithium chloride (5 wt%), and dry NMP (5.0 mL) were added at room temperature. To this solution, mPDA$_2$CyC$_2$ (0.439 g, 1.00 mmol) was added, and the mixture was stirred for 10 minutes, followed by stirring at 150 °C for 6 hours. The polymerization solution was then cooled to room temperature and poured into an excess amount of methanol (300 mL) containing NH_3 (aq.) (3 mL) to remove HCl and inorganic salts produced during the reaction. The precipitate was washed with hot methanol and dried at 180 °C for 12 hours under reduced pressure. This procedure yielded 0.403 g (85%) of the title polymer. FT-IR [KBr (cm^{-1})]: 3616, 3381 (N–H), 3330–2896 (N–H, H-bonded), 1576 (C=N), 1508 (C=C), 1441 (C=N), 1400 (C=C), 1185, 1161 (C–N), 868, 801, 768, 677 (C–H). ^{1}H-NMR (400 MHz, DMSO-d_6, ppm) δ 6.76 (CH, 4H), 7.17 (CH, 3H), 7.58 (CH, 2H), 7.80 (aromatic CH, 2H), 8.23 (aromatic CH, 1H), 8.83 (guanamine NH, 2H), 8.90 (ring guanamine NH, 4H).

Poly(mPDA$_2$CyC$_2$-*p*PDA) (*c*-PG(*p*PDA))

A similar procedure described above was used except for using *p*PDA (0.108 g, 1.00 mmol) instead of *m*PDA. Yield 0.260 g (55%). FT-IR[KBr (cm^{-1})]: 3616, 3377 (N–H), 3330–3110 (N–H, H-bonded), 1579 (C=N), 1485 (C=C), 1441 (C=N), 1398 (C=C), 1200 (C–N), 864, 806, 768, 677 (C–H).

Poly(mPDA$_2$CyC$_2$-ODA) (*c*-PG(ODA))

A similar procedure described above was used except for using ODA (0.200 g, 1.00 mmol) instead of *m*PDA. Yield 0.515 g (91%). FT-IR[KBr (cm^{-1})]: 3612, 3389 (N–H), 3330–3110 (N–H, H-bonded), 1574 (C=N), 1494 (C=C), 1439 (C=N), 1405 (C=C), 1205 (C–O), 1159 (C–N), 869, 802, 764, 675 (C–H). ^{1}H-NMR (400 MHz, DMSO-d_6, ppm) δ 6.75 (aromatic CH, 4H), 6.92 (aromatic

 This journal is © The Royal Society of Chemistry 2020

Open Access Article. Published on 08 January 2020. Downloaded on 6/14/2026 1:09:49 PM.
This article is licensed under a Creative Commons Attribution-NonCommercial 3.0 Unported Licence.

CH, 4H), 7.15 (aromatic CH, 2H), 7.77 (aromatic CH, 2H), 7.85 (aromatic CH, 4H), 8.89 (ring guanamine NH, 4H), 9.03 (guanamine NH, 2H).

Poly(*m*PDA$_2$CyC$_2$-BAFL) (*c*-PG(BAFL))

A similar procedure described above was used except for using BAFL (0.348 g, 1.00 mmol) instead of *m*PDA. Yield 0.657 g (92%). FT-IR[KBr (cm^{-1})]: 3623, 3384 (N–H), 3330–3110 (N–H, H-bonded), 1573 (C=N), 1509 (C=C), 1445 (C=N), 1412 (C=C), 1228, 1188, 1165 (C–N), 873, 808, 745, 680 (C–H). ^{1}H-NMR (400 MHz, DMSO-d_6, ppm) δ 6.71 (aromatic CH, 4H), 7.03 (aromatic CH, 4H), 7.12 (aromatic CH, 2H), 7.32–7.45 (aromatic CH, 6H), 7.73 (aromatic CH, 6H), 7.91 (aromatic CH, 2H), 8.85 (ring guanamine NH, 4H), 9.05 (guanamine NH, 2H).

Poly(*m*PDA$_2$CyC$_2$-TFMB) (*c*-PG(TFMB))

A similar procedure described above was used except for using TFMB (0.320 g, 1.00 mmol) instead of *m*PDA. Yield 0.570 g (83%). FT-IR[KBr (cm^{-1})]: 3645, 3402 (N–H), 3330–3110 (N–H, H-bonded), 1571 (C=N), 1513 (C=C), 1445 (C=N), 1404 (C=C), 1315, 1164 (C–N), 1113 (C–F), 870, 804, 760, 684 (C–H). ^{1}H-NMR (400 MHz, DMSO-d_6, ppm) δ 6.80 (aromatic CH, 4H), 7.23 (aromatic CH, 4H), 7.76 (aromatic CH, 2H), 8.04 (aromatic CH, 2H), 8.53 (aromatic CH, 2H), 9.06 (ring guanamine NH, 4H), 9.49 (guanamine NH, 2H).

Poly(*m*PDA$_2$CyC$_2$-BisAAF) (c-PG(BisAAF))

A similar procedure described above was used except for using BisAAF (0.334 g, 1.00 mmol) instead of *m*PDA. Yield 0.588 g (84%). FT-IR[KBr (cm^{-1})]: 3604, 3399 (N–H), 3330–3110 (N–H, H-bonded), 1576 (C=N), 1510 (C=C), 1447 (C=N), 1406 (C=C), 1238 (C–F), 1196, 1164 (C–N), 963, 924 (C–CF$_3$), 802 (C–H). ^{1}H-NMR (400 MHz, DMSO-d_6, ppm) δ 6.76 (aromatic CH, 4H), 7.16 (aromatic CH, 2H), 7.23 (aromatic CH, 4H), 7.78 (aromatic CH, 2H), 8.03 (aromatic CH, 4H), 8.99 (ring guanamine NH, 4H), 9.36 (guanamine NH, 2H).

Film preparation

The polymer sample was dissolved in DMAc (5 wt%), and the homogeneous solution was drop-cast onto a glass plate. After drying in an oven at room temperature for 12 hours, the film was sequentially dried at temperatures of 50 °C, 80 °C, and 120 °C for 3 hours each. Finally, the film was dried at 150 °C for 12 hours.

Measurements

FT-IR spectra were recorded on a JASCO FT/IR-4200 using the KBr pellet method. NMR spectroscopy was performed on a Bruker AC-400P spectrometer at 400 MHz for ^{1}H and 100 MHz for ^{13}C measurements. Deuterated dimethyl sulfoxide (DMSO-d_6) was used as the solvent, with tetramethylsilane as the internal reference. The M_n, M_w, and M_w/M_n values were determined using a Tosoh HLC-8220 gel permeation chromatograph equipped with refractive index and UV detectors and a consecutive polystyrene gel column (TSK-GEL α-M $\times$2) at 40 °C and eluted with NMP containing 0.01 mol L^{-1} LiBr at a flow rate of 1.0 mL min^{-1}. Thermogravimetric analysis was performed on a Hitachi TG/DTA7220 system at a heating rate of 10 °C min^{-1} under exposure to air or N_2. Differential scanning calorimetry (DSC) was performed on a Hitachi X-DSC7000 system at a heating rate of 20 °C min^{-1} under nitrogen. Thermal mechanical analysis (TMA) was performed on a Hitachi TMA/SS7100 at a heating rate of 10 °C min^{-1} under nitrogen. Dynamic mechanical analysis (DMA) was performed on a Hitachi DMS7100 at a heating rate of 2 °C min^{-1} under nitrogen. Polymer films were cut into pieces of 20 mm $\times$ 9 mm $\times$ 0.12 mm dimensions, and a load was applied to the films with a strain amplitude of 5 μm and a frequency of 1 Hz. The tensile properties of the films were measured on an AGS-X (Shimadzu) at an extension rate of 10 mm min^{-1}. The optical transparency of the PG films was measured using a Shimadzu UV-vis spectrophotometer (UV-1800). Refractive index and birefringence were measured by Metricon Prism Coupler Model 2010/M. Fast-atom-bombardment mass spectroscopy was performed using a JEOL JMS-700 mass spectrometer. FAB was generated using xenon as the primary beam at 6 keV energy. The ion-accelerating voltage was 10 kV and 3-nitrobenzyl alcohol was used for the FAB ionization matrix.

Conflicts of interest

There are no conflicts to declare.

Acknowledgements

The authors thank Ms Shiduko Nakajo (Iwate University) for FAB MS measurements.

Notes and references

1 S. Kopolow, T. E. Hogen Esch and J. Smid, *Macromolecules*, 1971, **4**, 359–360.
2 M. J. Marsella and T. M. Swager, *J. Am. Chem. Soc.*, 1993, **115**, 12214–12215.
3 H. Cheng, L. Ma, Q. S. Hu, X. F. Zheng, J. Anderson and L. Pu, *Tetrahedron: Asymmetry*, 1996, **7**, 3083–3086.
4 N. Yamaguchi and H. W. Gibson, *Angew. Chem., Int. Ed.*, 1999, **38**, 143–147.
5 J. Morgado, F. Cacialli, R. H. Friend, B. S. Chuah, S. C. Moratti and A. B. Holmes, *Synth. Met.*, 2000, **111–112**, 449–452.
6 S. H. Liao, Y. L. Li, T. H. Jen, Y. S. Cheng and S. A. Chen, *J. Am. Chem. Soc.*, 2012, **134**, 14271–14274.
7 M. Furue, A. Harada and S. Nozakura, *J. Polym. Sci., Part C: Polym. Lett.*, 1975, **13**, 357–360.
8 S. Shinkai, H. Kawaguchi and O. Manabe, *J. Polym. Sci., Part C: Polym. Lett.*, 1988, **26**, 391–396.
9 *Calixarenes 2001*, ed. Z. Asfari, V. Böhmer, J. Harrowfield and J. Vicens, Kluwer Academic, Dordrecht, 2001.
10 C. D. Gutsche, Calixarenes: An Introduction, in *Monographs in Supramolecular Chemistry*, ed. J. F. Stoddart, The Royal Society of Chemistry, Cambridge, 2nd edn, 2008.

Open Access Article. Published on 08 January 2020. Downloaded on 6/14/2026 1:09:49 PM.
This article is licensed under a Creative Commons Attribution-NonCommercial 3.0 Unported Licence.

11 J. Ueda, M. Kamigaito and M. Sawamoto, *Macromolecules*, 1998, **31**, 6762–6768.
12 S. Angot, K. S. Murthy, D. Taton and Y. Gnanou, *Macromolecules*, 1998, **31**, 7218–7225.
13 A. I. Costa, L. F. V. Ferreira and J. V. Prata, *J. Polym. Sci., Part A: Polym. Chem.*, 2008, **46**, 6477–6488.
14 P. D. Barata, A. I. Costa, L. F. V. Ferreira and J. V. Prata, *J. Polym. Sci., Part A: Polym. Chem.*, 2010, **48**, 5040–5052.
15 P. D. Barata, A. I. Costa and J. V. Prata, *React. Funct. Polym.*, 2012, **72**, 627–634.
16 J. H. Wosnick and T. M. Swager, *Chem. Commun.*, 2004, 2744–2745.
17 A. I. Costa, H. D. Pinto, L. F. V. Ferreira and J. V. Prata, *Sens. Actuators, B*, 2012, **161**, 702–713.
18 P. D. Barata and J. V. Prata, *ChemPlusChem*, 2014, **79**, 83–89.
19 J. V. Prata, A. I. Costa, G. Pescitelli and H. D. Pinto, *Polym. Chem.*, 2014, **5**, 5793–5803.
20 A. Dondoni, C. Ghiglione, A. Marraa and M. Scoponi, *Chem. Commun.*, 1997, 673–674.
21 S. I. Kim, T. J. Shin, M. Ree, G. T. Hwang, B. H. Kim, H. Han and J. Seo, *J. Polym. Sci., Part A: Polym. Chem.*, 1999, **37**, 2013–2026.
22 H. H. Yu, B. Xu and T. M. Swager, *J. Am. Chem. Soc.*, 2003, **125**, 1142–1143.
23 Y. Yang and T. M. Swager, *Macromolecules*, 2006, **39**, 2013–2015.
24 Y. Yang and T. M. Swager, *Macromolecules*, 2007, **40**, 7437–7440.
25 M. X. Wang and H. B. Yang, *J. Am. Chem. Soc.*, 2004, **126**, 15412–15422.
26 B. Y. Hou, D. X. Wang, H. B. Yang, Q. Y. Zeng and M. X. Wang, *J. Org. Chem.*, 2007, **72**, 5218–5226.
27 D. W. Wang and M. M. Fisher, *J. Polym. Sci., Polym. Chem. Ed.*, 1983, **21**, 671–677.
28 N. Irles, J. Puiggalí and J. A. Subirana, *Macromol. Chem. Phys.*, 2001, **202**, 3316–3322.
29 Y. Shibasaki, T. Koizumi, N. Nishimura and Y. Oishi, *Chem. Lett.*, 2011, **40**, 1132–1134.
30 K. Saito, N. Nishimura, S. Sasaki, Y. Oishi and Y. Shibasaki, *React. Funct. Polym.*, 2013, **73**, 756–763.
31 A. Fujimori, S. Miura, T. Kikkawa and Y. Shibasaki, *J. Polym. Sci., Part B: Polym. Phys.*, 2015, **53**, 999–1009.
32 T. Kotaki, N. Nishimura, M. Ozawa, A. Fujimori, H. Muraoka, S. Ogawa, T. Korenaga, E. Suzuki, Y. Oishi and Y. Shibasaki, *Polym. Chem.*, 2016, **7**, 1297–1308.
33 S. Miura, Y. Shidara, T. Yunoki, M. A. A. Mamun, Y. Shibasaki and A. Fujimori, *Macromol. Chem. Phys.*, 2017, **218**, 1600520.
34 Y. Shibasaki, T. Kotaki, T. Bito, R. Sasahara, N. Idutsu, A. Fujimori, S. Miura, Y. Shidara, N. Nishimura and Y. Oishi, *Polymer*, 2018, **146**, 12–20.
35 R. Wang, C. Pellerin and O. Lebel, *J. Mater. Chem.*, 2009, **19**, 2747–2753.

This journal is © The Royal Society of Chemistry 2020